Title:

Regulatory T cells in skin facilitate epithelial stem cell differentiation

Abstract:

The maintenance of tissue homeostasis is critically dependent on the self-renewal and differentiation capacity of epithelial stem cells (SCs)[1,2]. How extrinsic signals, including tissue resident immune cells, govern SC behavior is largely unknown. We have previously observed that regulatory T cells (T_{regs}) in skin preferentially localize to hair follicles (HFs)[3,4], which house a major subset of skin SCs (HFSCs). HF regeneration is critically dependent on HFSCs[5]. Here, we mechanistically dissect the role of T_{regs} in HFSC biology. We found that T_{reg} abundance and activation state in skin precisely correlate with the synchronous HF cycle. Lineage-specific cell depletion revealed that T_{regs} are required for HF regeneration. T_{regs} preferentially localize to the bulge region of HFs and facilitate HF cycling by directly augmenting HFSC proliferation and differentiation. Transcriptional and phenotypic profiling of T_{regs} and HFSCs revealed that T_{regs} in skin preferentially express high levels of the Notch ligand family member, Jag1, and the Notch signaling pathway was significantly enhanced in HFSCs when T_{regs} were present. In functional experiments, expression of Jag1 in T_{regs} was required for HFSC function and efficient HF regeneration. Taken together, our work functionally dissects the role of T_{regs} in HF biology and establishes a mechanistic link between tissue resident immune cells and epithelial SCs. These findings have clinical implications in human diseases of HFs, such as Alopecia Areata (AA), where T_{regs} are thought to play a role in disease pathogenesis[6–8].

Hair follicles in mammalian skin undergo bouts of regeneration, cycling between highly synchronized phases of quiescence (telogen) and growth (anagen). Both epithelial intrinsic and extrinsic environmental signals regulate the coordinated activation of telogen HFs to enter anagen[9]. Two findings have raised the possibility that skin-resident immune cells, specifically T_{regs}, are involved in this process. First, T_{regs} are concentrated in the vicinity of follicular epithelium[3,4], where HFSCs take residence[10]. Second, genome wide association studies have linked single nucleotide polymorphisms in T_{reg}-associated genes to AA, a disorder of immune-mediated disruption of HF regeneration[6,7]. In addition, augmenting T_{regs} clinically has shown efficacy in treating patients with this disease[8]. However, the contribution of T_{regs} to HFSC biology, or the mechanisms underlying such a pathway of SC regulation, is currently unknown. To test the hypothesis that T_{regs} play a functional role in HF biology, we began by performing comprehensive immune profiling of T_{regs} in murine skin at specific stages of the synchronous HF cycle[11]. The proportion of $CD4^{+}Foxp3^{+}$ T_{reg} cells in skin draining lymph nodes (SDLNs) of adult C57BL/6 mice showed little variability (Fig. 1a). In contrast, T_{reg} percentages and abundance in dorsal skin fluctuated significantly at different stages of the HF cycle. T_{regs} were significantly more abundant in the telogen phase of the HF cycle when compared to anagen (Fig. 1b and Extended Data Fig. 1). In addition, the proliferative index and activation state of skin T_{regs} (as evidenced by expression of Ki67, CD25, ICOS, GITR, and CTLA-4) also correlated with stage of the HF cycle, as T_{regs} displayed a more activated phenotype in telogen skin (Extended Data Fig. 2).

Given that both T_{reg} abundance and activation correlated with HF stage, we sought to determine whether these cells play an active role in the process of HF cycling. To do so, we employed a well-characterized model of depilation-induced HF regeneration[11]. In this model, mice with dorsal skin HFs in telogen are depilated to remove hair shafts. This treatment rapidly initiates the telogen-to-anagen transition

homogenously across the entire depilated dorsum (anagen induction), and thus begins the process of hair regeneration. To determine if T_{regs} play a role in this process, we utilized mice transgenic for the diphtheria toxin receptor under the control of the Foxp3 promoter ($Foxp3^{DTR}$)[12]. These mice allow for robust depletion of T_{regs} following administration of Diphtheria toxin (DT). Importantly, T_{regs} begin to repopulate lymph nodes and peripheral tissues soon after the last DT treatment, permitting the study of transient T_{reg} loss at specific times during HF regeneration[12]. Ablation of T_{regs} markedly reduced hair regrowth when compared to wild type (WT) control mice treated with or without DT (Fig. 1c, d). Whereas control mice had complete hair regrowth by 14 days post-depilation, mice depleted of T_{regs} showed less than 20% regrowth at this time (Fig. 1d). In these initial experiments, T_{regs} were continually depleted (*i.e.,* DT administered every 2 days for 14 days). Because a major function of T_{regs} is to suppress inflammation, mice deficient in these cells for prolonged periods of time succumb to multi-organ autoimmunity[12]. Thus, we set out to determine whether attenuation of HF cycling in the absence of T_{regs} was simply a result of systemic inflammation. In addition, we wanted to precisely define a potential 'window' of time for T_{reg} requirement in HF cycling. To do so, we treated WT or $Foxp3^{DTR}$ mice with DT 'early' after depilation (up to 4 days post-depilation), 'late' after depilation (starting at 7 days post-depilation), or throughout the entire 14-day period of hair regeneration. Depletion of T_{regs} early after depilation completely recapitulated the attenuation of HF regeneration observed with constant T_{reg} depletion (Fig. 1e and Extended Data Fig. 3). In contrast, late T_{reg} depletion showed normal hair regrowth (Fig. 1e and Extended Data Fig. 3). Histologic examination of skin showed a marked diminution of anagen HFs in early T_{reg}-depleted mice. Whereas HFs in control mice displayed an elongated phenotype extending deep into the subcutaneous fat (indicative of anagen induction)[11], HFs from T_{reg}-depleted mice were significantly shorter in length and failed to extend beyond the superficial dermis (Fig. 1f, g and

Extended data Fig. 3). Taken together, these results indicate that activated T_{regs} are more abundant in telogen skin and that these cells play an essential role in the telogen-to-anagen transition of the HF cycle. Consistent with these findings, mice that lack all T cells ($Rag2^{-/-}$) have a significant delay in depilation-induced hair regeneration and anagen onset during the synchronous HF cycle (Extended Data Fig. 4).

Given that telogen HFs from T_{reg}-depleted mice failed to enter anagen after depilation, we sought to elucidate the cellular mechanisms responsible for this phenomenon. The HF bulge region is the best characterized niche for adult skin epithelial SC residence[10]. Activation of bulge HFSCs is required anagen onset[13,14]. Upon anagen induction, HFSCs are activated, begin to proliferate and eventually differentiate to form all cell lineages of the newly generated HF[15–17]. Because T_{regs} function early to facilitate anagen induction, we set out to determine their influence on HFSC activation during the telogen-to-anagen transition. To do so, we utilized a previously established flow cytometric approach to delineate HFSCs[18]. Epidermal cell suspensions were prepared from dorsal skin and stained for CD45, Sca-1, EpCAM, CD34 and integrin α6 (ITGA6). Bulge HFSCs were defined as $CD45^{neg}Sca\text{-}1^{neg}EpCAM^{low}CD34^{high}$ cells (Fig. 2a). High levels of ITGA6 expression on this population distinguishes basal bulge residing HFSCs from those in the suprabasal layer[17] (Fig. 2a). Analysis of mid-telogen WT skin confirmed the presence of quiescent bulge-resident HFSCs[10], as evidenced by lack of expression of the proliferative marker Ki67 (Fig. 2b, c). Consistent with previous reports[19], HFSC activation closely followed depilation-induced anagen, with an increased percentage of HFSCs expressing Ki67 4-days after depilation (Fig. 2b, c). Induction of HFSC proliferation was significantly reduced in mice depleted of T_{regs} in the early window of time after depilation (Fig. 2b, c). This proliferative defect appeared to be selective for the bulge HFSC compartment, as no difference in Ki67 expression was observed in non-bulge keratinocytes between T_{reg}-sufficient and T_{reg}-depleted mice (Fig. 2d). To

determine if T_{regs} play a similar role in the natural telogen-to-anagen transition of the HF cycle, we utilized Foxp3-Scurfy mice ($Foxp3^{Sf}$) that fail to develop functional Foxp3-expressing T_{reg} cells[20]. While WT littermate controls have entered 1st anagen on post-natal day 28, $Foxp3^{Sf}$ mice fail to do so, as evidenced by diminished proliferative potential of HFSCs, lack of dorsal skin pigmentation, and significantly reduced HF length (Extended Data Figure 5). These data suggest that T_{regs} are required to promote HFSC function during the normal cycle of hair follicle regeneration.

To elucidate how T_{regs} influence HFSC activation and differentiation, we performed whole transcriptome RNA sequencing (RNAseq) of bulge HFSCs. Lineage tracing studies in the SC niche have identified a role for basal cell progenitors and their progeny in adopting a HF fate[13,16,21–23]. We therefore sequenced $ITGA6^{high}$ basal bulge HFSCs purified from T_{reg}-sufficient and T_{reg}-depleted mice 4 days post-depilation. Consistent with our Ki67 flow cytometric data, there was a marked proliferative defect in HFSCs isolated from T_{reg}-depleted mice, as evidenced by a significant reduction in genes associated with cell proliferation (Supplementary Table 1). In addition, HFSCs isolated from T_{reg}-depleted mice showed a significant reduction in genes associated with differentiation to HF keratinocyte lineages[24] (Fig. 2e). Collectively, these results suggest that a major mechanism by which T_{regs} mediate anagen induction is through preferentially facilitating the activation and differentiation of bulge HFSCs.

T_{regs} are well known to play a major role in suppressing inflammation[25]. However, these cells have recently been show to have alternative functions in tissues, independent of their role in immunosuppression. In visceral adipose tissue, T_{regs} express the peroxisome proliferator-activated receptor-γ, enabling them to function in lipid and glucose metabolism[26]. In addition, T_{regs} in muscle and lung express high levels of the epidermal growth factor ligand, amphiregulin, giving them the ability to directly facilitate tissue repair[27,28]. Alternative functions of T_{regs} in skin are currently unknown. It is

therefore possible that T_{regs} produce factors that directly promote the activation and differentiation of HFSCs. Alternatively, T_{regs} may indirectly facilitate anagen entry by suppressing inflammatory cells in and around the HFSC niche[29]. To determine if suppression of inflammation was the dominant mechanism by which T_{regs} mediate HFSC activation, we comprehensively assessed the inflammatory response in skin of T_{reg} depleted mice early after anagen induction. Hallmarks of skin inflammation, such as epidermal hyperplasia and immune cell infiltrate, were not significantly different between control and T_{reg} depleted mice (Fig. 3a-b). In addition, absolute numbers of dermal γδ T cells, dendritic epidermal T cells, cytotoxic $CD8^+$ T cells, $CD4^+Foxp3^-$ T effector cells, $CD3^-γδ^-$ lineage negative cells, dendritic cells, neutrophils, and macrophages remained unchanged between T_{reg} depleted and T_{reg} sufficient mice during this acute anagen induction period (Fig. 3c and Extended Data Figure 6). Similarly, skin effector T cell production of the cytokines interleukin (IL)-22, interferon-γ (IFNγ), IL-17 and tumor necrosis factor-α were comparable between control and T_{reg} depleted mice (Fig. 3c-e and Extended Data Figure 6b-d), suggesting that the absence of T_{regs} during this defined window of anagen induction does not result in overt skin inflammation. To functionally test whether T_{regs} indirectly facilitate anagen onset by suppressing inflammatory cells, the major immune cell populations in skin were co-depleted with T_{regs} and the proliferative capacity of HFSCs in response to anagen induction was assayed. If T_{regs} facilitate HFSC activation by suppressing inflammatory cells, we would predict that co-depletion of these cells with T_{regs} would rescue depilation-induced HFSC proliferation. However, we observed that suppression of HFSC proliferation following T_{reg} depletion was not rescued by co-depletion of $CD4^+$ T cells, $CD8^+$ T cells, Gr-1 expressing myeloid cells, or CD11c-expressing myeloid cells (Fig. 3f). In addition, both antibody neutralization and genetic deletion of the interferon-γ pathway, a major effector cytokine suppressed by T_{regs}[30], did not rescue HFSC activation (Fig. 3f). These findings were

consistent with the lack of skin inflammation observed in our early transient T_{reg} ablation model (Fig. 3a-e). Taken together, these data suggest that suppression of local immune cells is not the dominant mechanism by which T_{regs} facilitate HFSC differentiation.

To determine if T_{regs} directly interact with HFSCs, we first set out to establish the extent of co-localization of these two cell populations. Immunofluorescence microscopy revealed that T_{regs} reside proximal to the lower portions of telogen HFs, clustering in close association with the bulge region (Fig. 3g). Co-staining of Foxp3 with Keratin-15 and ITGA6, markers of bulge resident SCs[16], revealed a sub-population of bulge-associated T_{regs} in direct interaction with HFSCs (Fig. 3h and Extended Data Figure 7). Cells that are in constant contact with other cells typically have characteristic dynamic behavior. Specifically, cell-to-cell contacts alter the shape of cells such that they are no longer spherical[31]. Thus, we hypothesized that bulge-associated T_{regs} would have fundamentally different cell shape and cell dynamics when compared to T_{regs} found outside this region. To test this, we developed a non-invasive vacuum suction approach for live intravital 2-photon imaging of T_{regs} in dorsal skin of $Foxp3^{GFP}$ reporter mice[32]. Utilizing this system, we observed that bulge-associated T_{regs} differ markedly with respect to shape and behavior when compared to T_{regs} found >20 μm away from follicular epithelium. Bulge-associated T_{regs} displayed a more amoeboid cell morphology with increased protrusive activity (Extended Data Figure 7 and Supplementary Video 1 and Video 2). This differential cell shape was quantified in individual skin T_{regs} by applying a measure of relative sphericity[33,34]. When compared to non-bulge T_{regs}, the sphericity of bulge-associated T_{regs} was significantly lower (Extended Data Figure 7), indicating the presence of a more dynamically active cell population in constant interaction with the HF milieu. Taken together with images obtained by static immunofluorescence microscopy, these observations suggest that T_{regs} directly interact with HFSCs in the bulge region of the HF.

We next set out to elucidate potential mechanisms by which T_{regs} may directly influence HFSC function. We hypothesized that pathways involved in this process would be preferentially expressed in skin T_{regs} when compared to T_{regs} found in SDLNs. Thus, we performed whole transcriptome RNA sequencing on T_{regs} purified from telogen skin and compared expression profiles to T_{regs} isolated from SDLNs (Supplementary Table 2). Consistent with heightened activation of T_{regs} in tissues[4,28,35], differential expression analyses revealed increased expression of genes associated with T_{reg} function in skin T_{regs} compared to SDLN T_{regs} (Fig. 4a). Most notably, Jag1, a ligand of the Notch signaling pathway, was among the highest differentially expressed genes between skin and SDLN T_{regs} (Fig. 4a). T_{regs} in skin expressed approximately 150-fold more Jag1 transcript than SDLN T_{regs} (p-value=$3.4x10^{-32}$; Fig. 4b). Assessment of Jag1 protein expression by flow cytometry confirmed preferential expression on skin T_{regs} relative to other adaptive immune cell populations in skin (Extended Data Figure 8). Aside from preferential expression on skin T_{regs}, this molecule was an especially interesting candidate given previous mechanistic studies identifying Jag1 and the canonical Notch signaling pathway as playing a major role in anagen induction and basal SC commitment to HF regeneration[15,36–38]. Having identified skin T_{reg} expression of Jag1, a known HF cycle inducer, we next sought to determine if Notch target gene transcripts[39] were differentially expressed in HFSCs in the presence of T_{regs}. Genome wide RNAseq analysis of HFSCs isolated 4 days after anagen induction in the presence or absence of T_{regs} revealed a differential signature of Notch target genes (Fig 4d, e). Of the 1174 differentially expressed genes between the two groups, 84 genes (~7%) were known transcriptional targets of the Notch signaling pathway (p-value of the overlap = $5.21x10^{-27}$). Collectively, these results indicate that T_{regs} in skin express high levels of the Notch ligand, Jag1, and that in the absence of T_{regs}, Notch signaling is attenuated in HFSCs. To functionally determine if Notch signaling plays a role in T_{reg}-mediated enhancement of

HFSC activation, we attempted to rescue the proliferative defect observed in HFSCs in T_{reg}-depleted mice by the exogenous addition of Jag1[40]. Microbeads coated with Jag1-Fc or control Fc were subcutaneously administered to DT-treated $Foxp3^{DTR}$ mice and activation of HFSCs was quantified by flow cytometry 4 days post-depilation. In these experiments, exogenous Jag1 was able to partially rescue HFSC activation and induction of anagen (as measured by HF length) imparted by the absence of T_{regs} (Fig. 4f, g).

To definitively test whether Jag1 expression on T_{regs} is required for anagen induction, mice expressing a Jag1 conditional allele[41] (*Jag1$^{fl/fl}$*) were crossed to *Foxp3-cre* mice[42] to specifically ablate Jag1 expression in T_{regs}. Early after anagen induction, $Foxp3^{Cre/Cre}Jag1^{fl/fl}$ mice had significantly attenuated proliferative capacity of integrin-$\alpha6^{high}$ $CD34^{+}$ bulge HFSCs when compared to age- and gender-matched littermate controls (Fig. 4h-i). In addition, we assessed the epidermal expression of key differentiation associated genes identified in our whole genome RNA-sequencing analysis. Relative to control mice, deletion of Jag1 in T_{regs} resulted in a significant reduction in the expression of Bgn, Ccnd1, Gdf10, Sox4, Sox7 and Timp3 (Fig. 4j). Given the early requirement for T_{regs} in HFSC activation, we then monitored these mice for the earliest clinical sign of anagen entry - dorsal skin pigmentation[11]. To determine the anagen induction capacity in the absence and presence of Jag1 on T_{regs}, $Foxp3^{Cre/Cre}Jag1^{fl/fl}$ and control mice were depilated and dorsal skin pigmentation was quantified. Consistent with the diminished proliferative and differentiation capacity of HFSCs, the pigmentation intensity of $Foxp3^{Cre/Cre}Jag1^{fl/fl}$ dorsal skin was significantly decreased relative to control dorsal skin (Fig. 4k, l), revealing an essential function for Jag1 expression on T_{regs} for anagen induction. Collectively, these findings suggest that T_{regs} in skin utilize the Notch pathway, at least in part, to directly augment HFSC proliferation and differentiation.

In recent years, there has been a growing appreciation that tissue resident immune cells contribute to homeostatic and wound-induced regeneration[2]. The non-immunologic functions of cutaneous T_{regs}, a major skin-resident immune cell population, have yet to be defined. Here, we identify a functional requirement of skin T_{regs} for the regeneration of HFs through enhancing bulge HFSC activation and differentiation. T_{reg}-mediated induction of SC activation provides a novel pathway by which an immune cell population influences SC behavior in tissues, with a marked impact on regeneration, and ultimately tissue function. These results also suggest that T_{reg} impairment may contribute to dysregulated HF cycling observed in patients with AA, establishing a foundation for new therapeutic strategies targeting this disease and potentially other tissue regenerative disorders.

Bibliography

1. Bergmann, A. & Steller, H. Apoptosis, stem cells, and tissue regeneration. *Sci. Signal.* **3,** re8 (2010).
2. Aurora, A. B. & Olson, E. N. Immune modulation of stem cells and regeneration. *Cell Stem Cell* **15,** 14–25 (2014).
3. Gratz, I. K. *et al.* Cutting Edge: memory regulatory t cells require IL-7 and not IL-2 for their maintenance in peripheral tissues. *J. Immunol. Baltim. Md 1950* **190,** 4483–4487 (2013).
4. Sanchez Rodriguez, R. *et al.* Memory regulatory T cells reside in human skin. *J. Clin. Invest.* **124,** 1027–1036 (2014).
5. Blanpain, C. & Fuchs, E. Epidermal homeostasis: a balancing act of stem cells in the skin. *Nat. Rev. Mol. Cell Biol.* **10,** 207–217 (2009).

6. Conteduca, G. *et al.* Single nucleotide polymorphisms in the promoter regions of Foxp3 and ICOSLG genes are associated with Alopecia areata. *Clin. Exp. Med.* **14,** 91–97 (2014).
7. Petukhova, L. *et al.* Genome-wide association study in alopecia areata implicates both innate and adaptive immunity. *Nature* **466,** 113–117 (2010).
8. Castela, E. *et al.* Effects of low-dose recombinant interleukin 2 to promote T-regulatory cells in alopecia areata. *JAMA Dermatol.* **150,** 748–751 (2014).
9. Plikus, M. V. & Chuong, C.-M. Macroenvironmental regulation of hair cycling and collective regenerative behavior. *Cold Spring Harb. Perspect. Med.* **4,** a015198 (2014).
10. Cotsarelis, G., Sun, T. T. & Lavker, R. M. Label-retaining cells reside in the bulge area of pilosebaceous unit: implications for follicular stem cells, hair cycle, and skin carcinogenesis. *Cell* **61,** 1329–1337 (1990).
11. Müller-Röver, S. *et al.* A comprehensive guide for the accurate classification of murine hair follicles in distinct hair cycle stages. *J. Invest. Dermatol.* **117,** 3–15 (2001).
12. Kim, J. M., Rasmussen, J. P. & Rudensky, A. Y. Regulatory T cells prevent catastrophic autoimmunity throughout the lifespan of mice. *Nat. Immunol.* **8,** 191–197 (2007).
13. Tumbar, T. *et al.* Defining the epithelial stem cell niche in skin. *Science* **303,** 359–363 (2004).
14. Greco, V. *et al.* A two-step mechanism for stem cell activation during hair regeneration. *Cell Stem Cell* **4,** 155–169 (2009).

15. Blanpain, C., Lowry, W. E., Pasolli, H. A. & Fuchs, E. Canonical notch signaling functions as a commitment switch in the epidermal lineage. *Genes Dev.* **20,** 3022–3035 (2006).

16. Morris, R. J. *et al.* Capturing and profiling adult hair follicle stem cells. *Nat. Biotechnol.* **22,** 411–417 (2004).

17. Trempus, C. S. *et al.* Enrichment for living murine keratinocytes from the hair follicle bulge with the cell surface marker CD34. *J. Invest. Dermatol.* **120,** 501–511 (2003).

18. Nagao, K. *et al.* Stress-induced production of chemokines by hair follicles regulates the trafficking of dendritic cells in skin. *Nat. Immunol.* **13,** 744–752 (2012).

19. Chen, T. *et al.* An RNA interference screen uncovers a new molecule in stem cell self-renewal and long-term regeneration. *Nature* **485,** 104–108 (2012).

20. Brunkow, M. E. *et al.* Disruption of a new forkhead/winged-helix protein, scurfin, results in the fatal lymphoproliferative disorder of the scurfy mouse. *Nat. Genet.* **27,** 68–73 (2001).

21. Ito, M. *et al.* Stem cells in the hair follicle bulge contribute to wound repair but not to homeostasis of the epidermis. *Nat. Med.* **11,** 1351–1354 (2005).

22. Levy, V., Lindon, C., Harfe, B. D. & Morgan, B. A. Distinct stem cell populations regenerate the follicle and interfollicular epidermis. *Dev. Cell* **9,** 855–861 (2005).

23. Jaks, V. *et al.* Lgr5 marks cycling, yet long-lived, hair follicle stem cells. *Nat. Genet.* **40,** 1291–1299 (2008).

24. Lowry, W. E. *et al.* Defining the impact of beta-catenin/Tcf transactivation on epithelial stem cells. *Genes Dev.* **19,** 1596–1611 (2005).

25. Sakaguchi, S., Yamaguchi, T., Nomura, T. & Ono, M. Regulatory T cells and immune tolerance. *Cell* **133,** 775–787 (2008).

26. Cipolletta, D. *et al.* PPAR-γ is a major driver of the accumulation and phenotype of adipose tissue Treg cells. *Nature* **486,** 549–553 (2012).

27. Arpaia, N. *et al.* A Distinct Function of Regulatory T Cells in Tissue Protection. *Cell* **162,** 1078–1089 (2015).

28. Burzyn, D. *et al.* A special population of regulatory T cells potentiates muscle repair. *Cell* **155,** 1282–1295 (2013).

29. Paus, R., Nickoloff, B. J. & Ito, T. A 'hairy' privilege. *Trends Immunol.* **26,** 32–40 (2005).

30. Sojka, D. K. & Fowell, D. J. Regulatory T cells inhibit acute IFN-γ synthesis without blocking T-helper cell type 1 (Th1) differentiation via a compartmentalized requirement for IL-10. *Proc. Natl. Acad. Sci. U. S. A.* **108,** 18336–18341 (2011).

31. Lecuit, T. & Lenne, P.-F. Cell surface mechanics and the control of cell shape, tissue patterns and morphogenesis. *Nat. Rev. Mol. Cell Biol.* **8,** 633–644 (2007).

32. Lin, W. *et al.* Regulatory T cell development in the absence of functional Foxp3. *Nat. Immunol.* **8,** 359–368 (2007).

33. Zaid, A. *et al.* Persistence of skin-resident memory T cells within an epidermal niche. *Proc. Natl. Acad. Sci. U. S. A.* **111,** 5307–5312 (2014).

34. Matheu, M. P. *et al.* Three phases of CD8 T cell response in the lung following H1N1 influenza infection and sphingosine 1 phosphate agonist therapy. *PloS One* **8,** e58033 (2013).

35. Feuerer, M. *et al.* Lean, but not obese, fat is enriched for a unique population of regulatory T cells that affect metabolic parameters. *Nat. Med.* **15,** 930–939 (2009).

36. Estrach, S., Ambler, C. A., Lo Celso, C., Hozumi, K. & Watt, F. M. Jagged 1 is a beta-catenin target gene required for ectopic hair follicle formation in adult epidermis. *Dev. Camb. Engl.* **133,** 4427–4438 (2006).

37. Pan, Y. *et al.* gamma-secretase functions through Notch signaling to maintain skin appendages but is not required for their patterning or initial morphogenesis. *Dev. Cell* **7,** 731–743 (2004).

38. Vauclair, S., Nicolas, M., Barrandon, Y. & Radtke, F. Notch1 is essential for postnatal hair follicle development and homeostasis. *Dev. Biol.* **284,** 184–193 (2005).

39. Meier-Stiegen, F. *et al.* Activated Notch1 target genes during embryonic cell differentiation depend on the cellular context and include lineage determinants and inhibitors. *PloS One* **5,** e11481 (2010).

40. Vas, V., Szilágyi, L., Pálóczi, K. & Uher, F. Soluble Jagged-1 is able to inhibit the function of its multivalent form to induce hematopoietic stem cell self-renewal in a surrogate in vitro assay. *J. Leukoc. Biol.* **75,** 714–720 (2004).

41. Brooker, R., Hozumi, K. & Lewis, J. Notch ligands with contrasting functions: Jagged1 and Delta1 in the mouse inner ear. *Dev. Camb. Engl.* **133,** 1277–1286 (2006).

42. Rubtsov, Y. P. *et al.* Regulatory T cell-derived interleukin-10 limits inflammation at environmental interfaces. *Immunity* **28,** 546–558 (2008).

43. Scharschmidt, T. C. *et al.* A Wave of Regulatory T Cells into Neonatal Skin Mediates Tolerance to Commensal Microbes. *Immunity* **43,** 1011–1021 (2015).

44. de Hoon, M. J. L., Imoto, S., Nolan, J. & Miyano, S. Open source clustering software. *Bioinforma. Oxf. Engl.* **20,** 1453–1454 (2004).

45. Reich, M. *et al.* GenePattern 2.0. *Nat. Genet.* **38,** 500–501 (2006).

46. Friedman, R. S., Beemiller, P., Sorensen, C. M., Jacobelli, J. & Krummel, M. F. Real-time analysis of T cell receptors in naive cells in vitro and in vivo reveals flexibility in synapse and signaling dynamics. *J. Exp. Med.* **207,** 2733–2749 (2010).

47. Thornton, E. E. *et al.* Spatiotemporally separated antigen uptake by alveolar dendritic cells and airway presentation to T cells in the lung. *J. Exp. Med.* **209,** 1183–1199 (2012).

Figure Legends

Figure 1. T_{regs} are required for hair regeneration. a, T_{reg} cell abundance in skin draining lymph nodes (SDLNs) and skin of adult 4-14 week old WT mice as measured by flow cytometry. Pre-gated on live $CD45^+CD3^+CD4^+$ cells. **b**, Flow cytometric quantification of skin T_{regs} from dorsal skin of C57BL/6 mice at specific stages of the synchronous HF cycle (*n* = 5-12 mice per time point). $Foxp3^{DTR}$ mice or control WT mice were treated with DT on days -2, -1, and depilated on day 0 to induce anagen. DT administration was continued from Day 1 and then every other day until the termination of the experiment at day 14. **c**, Representative photos and (**d**) kinetics of hair regrowth in WT and T_{reg} depleted ($Foxp3^{DTR}$) mice (*n* = 3-4 mice per group). T_{regs} were depleted either up to day 4 (early), from day 7 onwards (late) or constitutively (con) throughout the experimental period. **e**, Hair regrowth at day 14 in WT and $Foxp3^{DTR}$ mice with DT treatments as indicated. **f**, Representative H&E staining of skin from WT and $Foxp3^{DTR}$ mice on day 14. Arrows indicate anagen HF extension into subcutaneous fat. Scale Bars, 100 μm. **g**, Quantification of HF length on day 14 by line measurement tool from image acquisition software, Zen (Zeiss). Data are mean ± s.e.m. **** P<0.0001, Student's *t*-test.

Figure 2. T_{regs} are required for HFSC proliferation and differentiation. a, Flow cytometric gating strategy to identify $CD34^+$ integrin $\alpha6^{high}$ (ITGA6) bulge HFSCs. $Foxp3^{DTR}$ mice or control mice were treated with DT on days -2, -1, depilated on day 0 to induce anagen and DT administered again on days 1 and 3 (*i.e.,* early regimen) . **b**, Representative flow cytometric plots of Ki67 expression in bulge HFSCs between WT and $Foxp^{DTR}$ mice 4 days after depilation. **c**, Flow cytometric quantification of $Ki67^+$ bulge HFSCs and (**d**) non-bulge keratinocytes 4 days after depilation. RNA sequencing was

performed on FACS purified bulge HFSCs at day 4 post-depilation from control (WT) or T_{reg} depleted ($Foxp3^{DTR}$) mice. **e**, Fold change in HFSC differentiation genes in WT and $Foxp^{DTR}$ mice, expressed as fold change relative to WT (where a value of 1 = no change). Genes to the left of the solid line represent control genes. Significance values are calculated based on transcript expression level. Data are mean ± s.e.m. **** P<0.0001, ns = no significant difference, Student's *t*-test.

Figure 3. T_{regs} facilitate HFSC activation independently of suppressing skin inflammation. Control wild-type (WT) or $Foxp3^{DTR}$ mice were depilated and treated with DT according to the 'early' depletion protocol. **a**, total dermal infiltrate and (b) epidermal hyperplasia in DT treated control (WT + DT) and T_{reg} depleted ($Foxp3^{DTR}$ + DT) Dorsal skin on day 4 as measured by routine histology. **c**, The absolute cell number of innate and adaptive immune cell subsets in skin as measured by flow cytometry. **d**, The proportion of cytokine producing $CD4^+$ T_{eff} Cells, and (e) $CD8^+$ T cells in dorsal skin. **f**, Flow cytometric quantification of $Ki67^+$ bulge HFSCs at day 4 post-depilation in immune cell depleted and interferon-γ neutralized (or interferon-γ signaling deficient) mice. **g**, Representative immunofluorescent image of $Foxp3^+$ T_{regs} in telogen skin of $Foxp3^{GFP}$ reporter mice. Dashed line indicates outline of HF. 'B' indicates bulge region. **h**, T_{reg} cell co-staining with Keratin-15. Scale Bars, 50 μm. One representative experiment of two, with *n* = 3-4 mice per group (a-e). Combined data from two experiments (f). Data are mean ± s.e.m. ns = no significant difference, Student's *t*-test.

Figure 4. T_{reg} expression of Jagged-1 (Jag1) is required for efficient HFSC activation and anagen induction. RNA sequencing was performed on telogen skin

T_{regs} and T_{regs} isolated from SDLNs. **a,** Volcano plot comparing expression profile of skin versus SDLN T_{regs}. **b**, Raw gene counts of Jag1 transcripts as quantified by RNA sequencing (n = 4 for skin T_{regs} and n = 3 for SDLN T_{regs}). RNA sequencing was performed on FACS purified bulge HFSCs at day 4 post-depilation from control (WT) or T_{reg} depleted ($Foxp3^{DTR}$) mice. **c**, Hierarchial clustering of differential expression of Notch target genes in HFSCs sequenced from control (WT) and T_{reg} depleted (DTR) mice, depicted as a heat map **d**, Venn diagram depicting the overlap between the total differentially expressed (DE) genes and known Notch target genes. P-value represents the significance of the overlap as determined by a chi-squared test. Jag1-Fc coated or control Fc coated beads were administered subcutaneously in T_{reg} depleted mice on days -2, -1, 1 and 3. All mice were depilated on day 0. **e**, Representative flow cytometric plots 4 days post-depilation gated on HFSCs from WT and $Foxp3^{DTR}$ mice treated with control or Jag1-Fc coated beads. **f**, Quantification of $Ki67^{+}$ bulge HFSCs and (g) HF length 4 days post-depilation. Control (*i.e.,* $Foxp3^{Cre/Cre}Jag1^{wt/wt}$ or $Foxp3^{wt/wt}Jag1^{fl/fl}$) or $Foxp3^{Cre/Cre}Jag1^{fl/fl}$ mice were depilated to induce anagen. **h**, Representative flow cytometric plots and **i**, quantification of $Ki67^{+}$ bulge HFSCs **j**, Fold change in HFSC differentiation genes as measured by qRT-PCR. **k**, Representative photos and (**l**) quantification of skin pigmentation. RNA-Seq experiments were conducted using 2-4 biological samples (a-d). Data are combined from three independent experiments (e-g). One representative experiment of two (h-l). Data are mean ± s.e.m. *P<0.05, **P<0.01 ***P<0.001, ****P<0.001, Student's *t*-test.

Rosenblum 2015-12-16763B
Figure 1

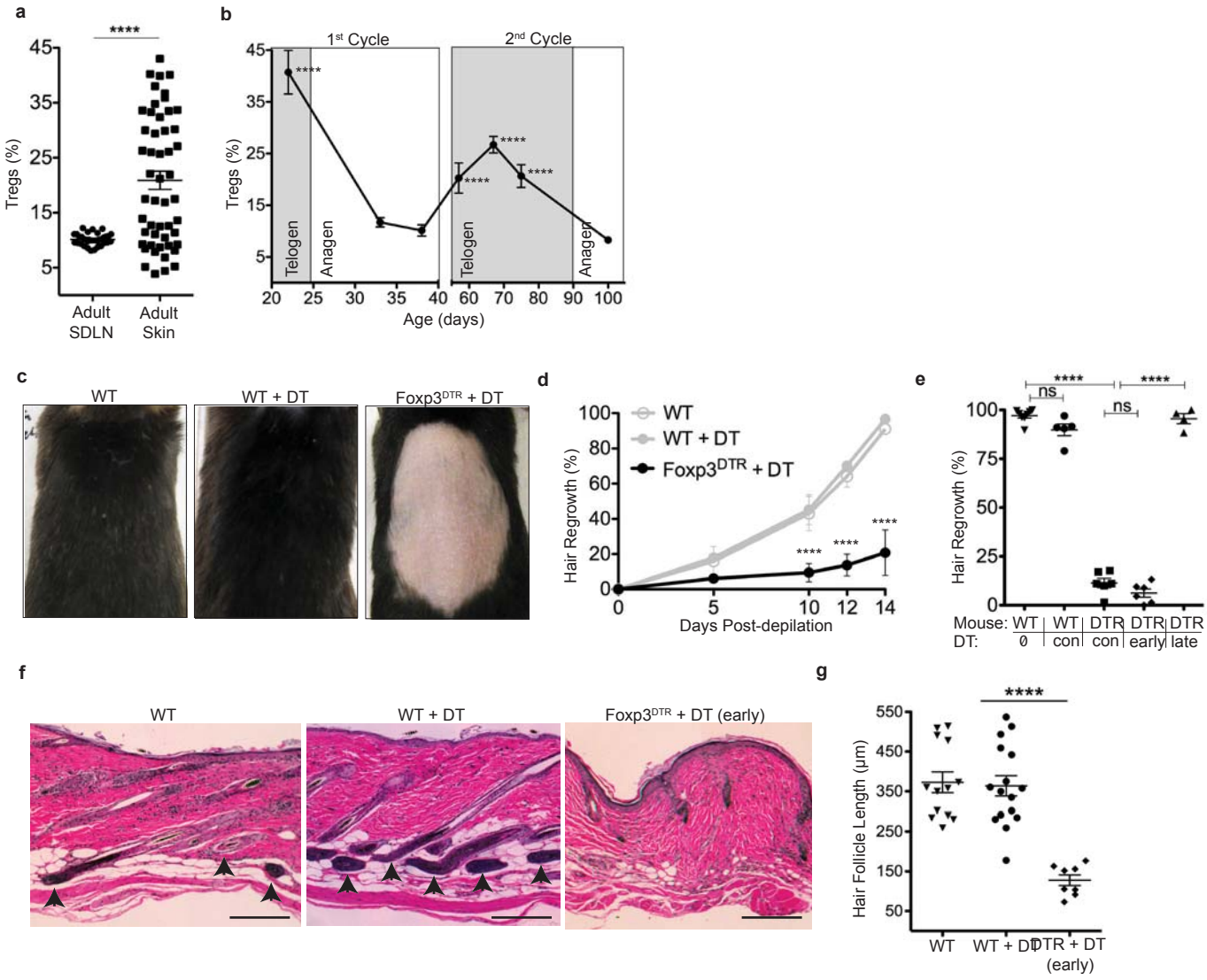

Rosenblum 2015-12-16763B
Figure 2

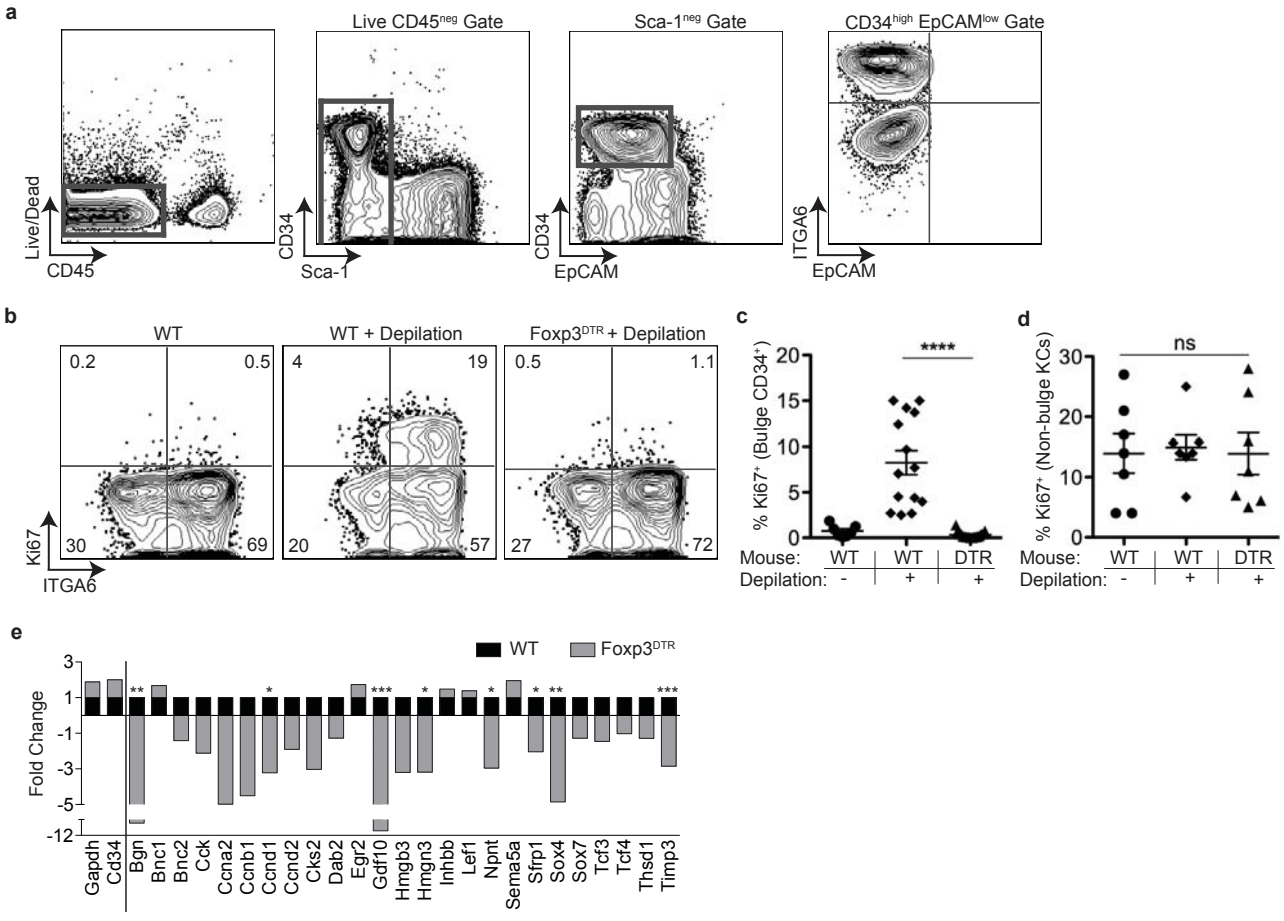

Rosenblum 2015-12-16763B
Figure 3

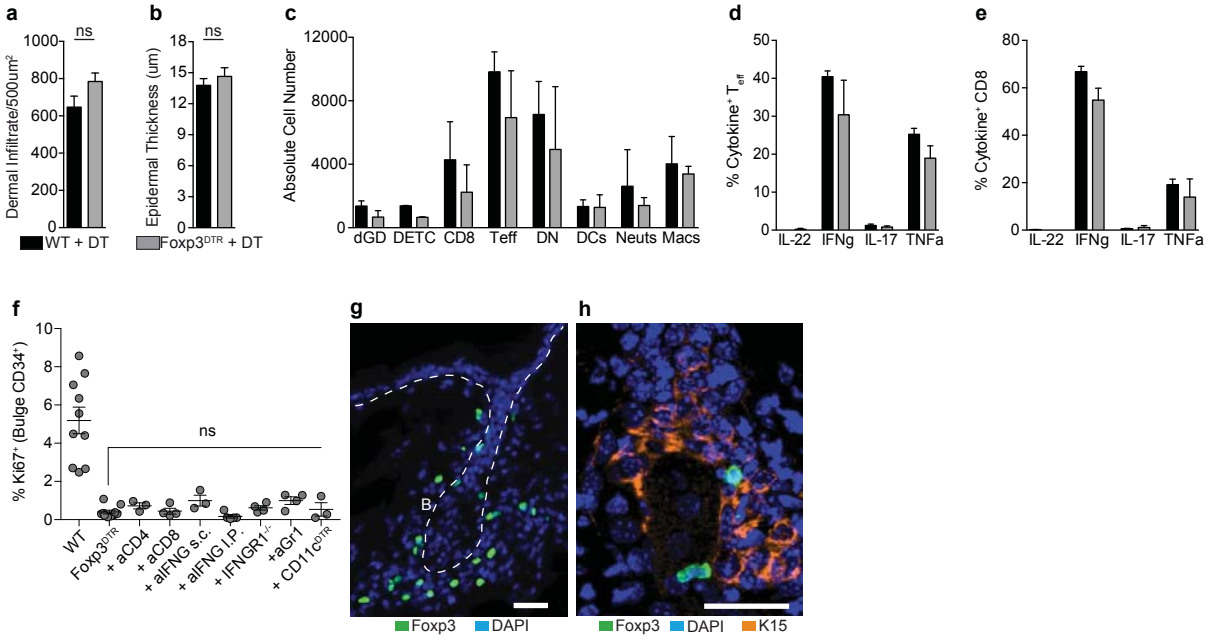

Rosenblum 2015-12-16763B
Figure 4